

A Planar Source of Atmospheric-Pressure Plasma Jet

O. S. Zhdanova^{a, *}, V. S. Kuznetsov^{b, c}, V. A. Panarin^b, V. S. Skakun^b,
E. A. Sosnin^{b, c}, and V. F. Tarasenko^b

^a Siberian State Medical University, Tomsk, 634050 Russia

^b Institute of High Current Electronics, Siberian Branch, Russian Academy of Sciences, Tomsk, 634055 Russia

^c Tomsk State University, Tomsk, 634050 Russia

*e-mail: badik@loi.hcei.tsc.ru

Received February 19, 2016

Abstract—In a single-barrier discharge with voltage sharpening and low gas consumption (up to 1 L/min), plane atmospheric pressure plasma jets with a width of up to 3 cm and length of up to 4 cm in air are formed in the slit geometry of the discharge zone. The energy, temperature, and spectral characteristics of the obtained jets have been measured. The radiation spectrum contains intense maxima corresponding to vibrational transitions of the second positive system of molecular nitrogen N_2 ($C^3\Pi_u \rightarrow B^3\Pi_g$) and comparatively weak transition lines of the first positive system of the N_2^+ ion ($B^2\Sigma_u^+ \rightarrow X^2\Sigma_g$). By an example of inactivation of the *Staphylococcus aureus* culture (strain ATCC 209), it is shown that plasma is a source of chemically active particles providing the inactivation of microorganisms.

DOI: 10.1134/S1063780X18010166

INTRODUCTION

Sources of atmospheric pressure plasma jets (APPJs) became an object of extensive studies after understanding their applicability in biology, medicine, and machining of surfaces of different materials [1–3]. The plasma flow in different APPJ sources is formed as a rule in the discharge gap (the excitation is implemented by a radio frequency, corona, glow, or dielectric barrier discharge (DBD)) and then is pushed out through a narrow capillary or slit due to the excessive pressure in the discharge zone as compared to the atmospheric pressure [1–12]. Excitation by a glow, corona, or DBD creates nonequilibrium plasma with an average gas temperature from 20 to 400°C and charged particle density typical of weakly ionized gases (no higher than 10^{11} – 10^{12} cm⁻³) and active particle density of up to 100 ppm.

At temperatures close to room temperature, the plasma is called cold atmospheric plasma or nonthermal plasmas [2].

At present, APPJ sources in which helium, argon, and/or their mixtures with nitrogen play the part of a working gas came into common use. Forming an APPJ in nitrogen and air is much more difficult. In this case, there appear more chemically active particles [9], but the plasma flow becomes sensitive to the gas circulation rate and its temperature increases. Therefore, the plasma source cannot be treated as a low-temperature source any longer. It is also important that an extended plasma jet cannot be formed [12].

The glow is formed only in the near-electrode zone and rapidly decays in the free space beyond it.

In [13, 14], we proposed and studied a capillary DBD-based APPJ source forming stable flows with a length of up to 4 cm in air and nitrogen at atmospheric pressure. For this purpose, we used a scheme in which the voltage is significantly sharpened on the working gap (as compared to traditional schemes containing a dielectric barrier and a pin electrode) and the gas consumption is reduced to ~0.5 L/min. Under these conditions, the upper states of nitrogen are populated better and their quenching decreases. Correspondingly, plasma bunches (bullets) forming in a pulse discharge have time to run a larger distance before the decay, which just provides the formation of an extended plasma flow at the exit from the nozzle. On the whole, they are commonly treated as a plasma jet although it is not quite correct because it is formed discretely, i.e., not as in dc plasmotrons [2].

The aim of this work is to study the possibility of the change from the capillary geometry of the DBD APPJ source to the planar geometry, which can potentially expand application areas of the source.

EXPERIMENTAL SETUP AND MEASUREMENT TECHNIQUES

A planar plasma jet was obtained using a scheme shown in Fig. 1. For this purpose, air was supplied into quartz tube 1 from distributor 2. Tube 1 with a diame-

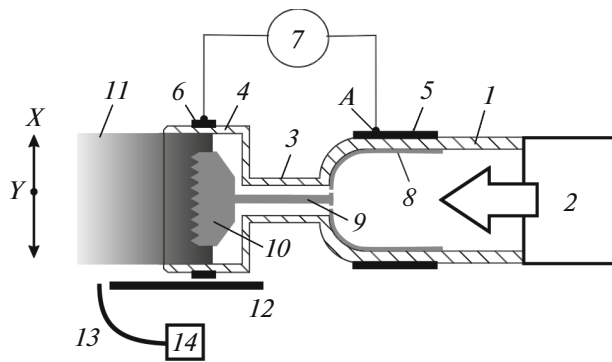


Fig. 1. Basic diagram of the setup and measurement scheme: (1, 3, 4) quartz elements, (2) gas supply, (5) high-voltage electrode, (6) ground electrode, (7) generator, (8–10) elements of the inner electrode, (11) plasma, (12) shielding shutter, (13) optical fiber, and (14) spectrometer. A heat-sensing device (not shown in the figure) or a photodetector was moved along the X and Y axes. The time behavior of the voltage was measured at point A .

ter of 41 mm had restriction 3 (with an inner diameter of 3.7 mm), which then passed into plane part 4 forming a plane slit with a thickness of 0.5 mm and length of 30 mm. On the outer surface of this element, two electrodes were positioned: ring high-voltage electrode 5 and grounded plane electrode 6. The electrodes were joined to generator 7. The setup also contained an internal electrode consisting of copper foil 8 tightly close to the inner part of tube 1 joined via 0.5-mm-thick transition conductor 9 with plane stainless-steel electrode 10 with a thickness of $\sim 150 \mu\text{m}$. The last electrode, with dimensions of $25 \times 12 \text{ mm}$, had several 2-mm-deep tip-shaped bumps with a step of 2 mm. However, both the number of bumps and their size, as well as the distance to the free space from them, were varied in the experiments.

During supply of a positive polarity voltage pulse to electrode 5, the wall of tube 1 is recharged and electrode 8 is charged. The geometric parameters of the source are such that the discharge takes place in the cavity between electrode 10 and dielectric part 4. As a result, plasma flow 11 appears at the exit from the slit. Along the X and Y axes, a heat-sensing device (not shown in the figure) or a photodetector was moved.

The power supply allowed one to vary the duration of the voltage pulse $\tau = 1\text{--}1.5 \mu\text{s}$, pulse repetition rate $f = 10\text{--}90 \text{ kHz}$, and voltage amplitude U of up to 10 kV.

The rate of gas pumping through the system was determined by the rate of filling test volumes placed on the plane slit of the source. The gas consumption was fixed under conditions favorable for the jet outflow from the exit slit; usually, it amounted to $0.95 \pm 0.1 \text{ L/min}$.

The radiation spectrum of the plasma at the exit was measured from different zones shielded by shutter 12 through optic fiber 13 with a known transmission spectrum, the signal from which was received

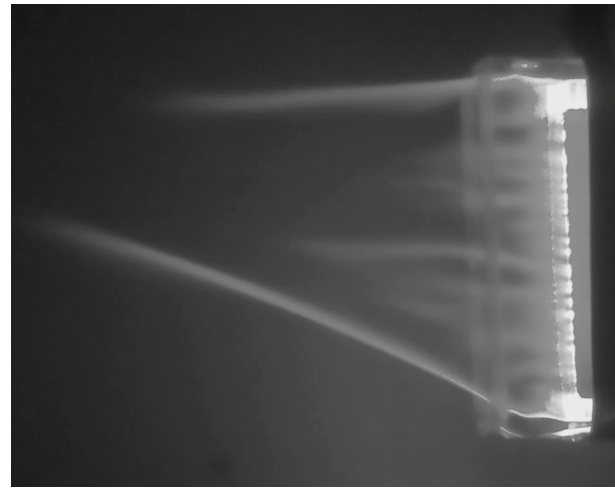


Fig. 2. Typical form of a planar glowing plasma stream at the exit from the slit ($f = 90 \text{ kHz}$, $U_A = 9.2 \text{ kV}$).

by an HR2000+ES spectrometer (Ocean Optics, Inc.) based on a Sony IL X511B multichannel CCD array (the operation range is 200–1100 nm and the full width at half-maximum of the instrumental function is 1.33 nm).

The plasma flow temperature on the X and Y axes (Fig. 1) was measured using a Pt1000 platinum temperature detector. For this purpose, at the first stage, the temperature was determined by the formula

$$t_1 = \frac{R_t - 100}{A}, \quad (1)$$

where R_t is the measured resistance of the detector and A is a constant coefficient (0.39692). At the next stage, the exact temperature was calculated by the formula

$$t_n = \frac{-((100t_{n-1}B + A)t_{n-1} + 100) + R_t}{A} + t_{n-1}, \quad (2)$$

where t_{n-1} is the temperature determined at the previous stage and B is a constant coefficient (5.8290×10^{-7}) [15].

The radiation power of the planar APPJ source was measured by a Hamamatsu H8025-222 photodetector, which was placed on the X and Y axes (Fig. 1) of the plasma flow and thermally isolated from the plasma by a quartz plate (not shown in Fig. 1).

RESULTS AND DISCUSSION

A typical appearance of a luminous stream is shown in Fig. 2. Depending on the applied voltage, the glow is either homogeneous or is divided into separate jets and the flow length amounts from 0.5 to 4 cm.

An example of the spatial distribution of the temperature at a distance of 5 mm from the exit slit in two axial directions X and Y is given in Fig. 3. It is seen that an increase in the pulse repetition rate from 30 to

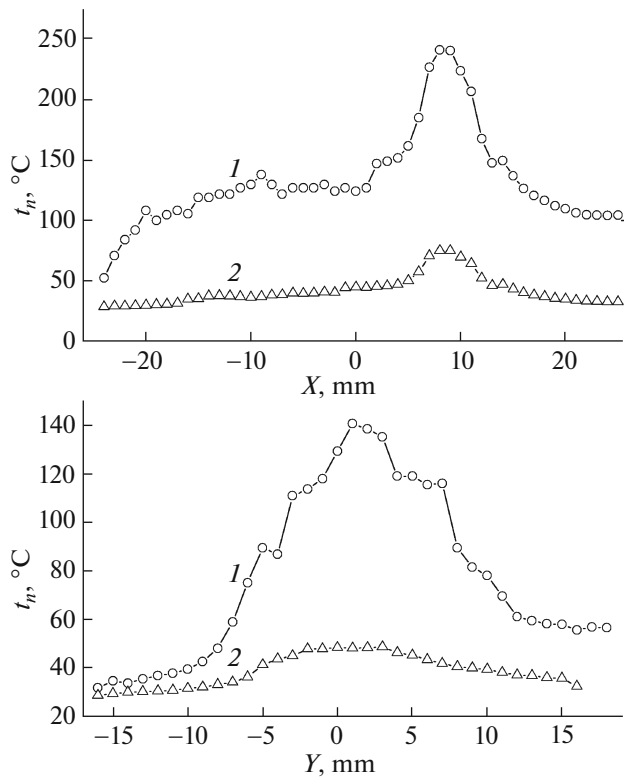


Fig. 3. Spatial distribution of the APPJ temperature in air along the X and Y axes at $U_A = 9.5$ kV for different repetition rates of voltage pulses: (1) 90 and (2) 30 kHz.

90 kHz leads to an approximately threefold increase in the plasma temperature for both longitudinal (X) and transverse (Y) directions of scanning by the temperature detector. The asymmetry of the temperature profiles is related to inhomogeneity of the plasma flow (see Fig. 2). These measurements allowed us to choose conditions for studying the inactivating action of the planar APPJ on the culture of *Staphylococcus aureus*, i.e., a regime that excludes the thermal factor of the inactivation.

The spectral investigations revealed the following: intensity maxima in the spectrum of a planar APPJ in air, namely, in the interval $\lambda = 280\text{--}460$ nm, correspond to vibronic transitions of the second positive system of molecular hydrogen N_2 ($C^3\Pi_u \rightarrow B^3\Pi_g$). In the spectrum, one can also observe weak lines corresponding to transitions of the first positive system of the N_2^+ ion ($B^2\Sigma_u^+ \rightarrow X^2\Sigma_g$) at wavelengths of 391 and 428 nm. These lines are well known in the literature (see references in [16]).

On the basis of its characteristics, the described plasma was treated as potentially able to inactivate microorganisms [17]. For this reason, pilot tests of its inactivating action were carried out.

As an object of treatment, the *Staphylococcus aureus* culture (strain ATCC 209) was taken. For this

purpose, a suspension of diurnal cultures in concentration of 2×10^4 CFU/mL was inoculated on Petri dishes with a growth medium. The experimental dishes were treated in air for different time at a distance of 45 mm from the exit slit. At this distance, one could exclude the action of heat (which was specially tested) and UV radiation of plasma (the energetic irradiance at the abovementioned distance was several tens of $\mu\text{W}/\text{cm}^2$). In other words, one could assume that the processing was carried out by chemical particles formed under conditions of an electric discharge in air. Most probably, these are nitrogen oxides, not ozone, because heating of the exit node (see Fig. 1) and narrow width of the slit must lead to fast recombination of ozone. This is verified by the disappearance of the ozone odor after ~ 90 s after the plasma source is switched on, which is usually sufficient to warm up the working area of the discharge.

The processed dishes, together with unprocessed control dishes, were placed in a thermostat. Then, the grown colonies were counted and compared with the control group.

As a result, the obtained values for the exposure times of 15, 30, and 120 s were $(0.14 \pm 0.08) \times 10^3$, $(0.24 \pm 0.11) \times 10^3$, and $(0.25 \pm 0.12) \times 10^3$ CFU, respectively. Thus, it has been demonstrated that the concentration of viable microorganisms was reduced approximately by an order of magnitude regardless of time. This corroborates the fact that the developed APPJ source is able to create chemically active particles.

CONCLUSIONS

A new source of planar atmospheric-pressure plasma jets has been proposed and evaluated. The construction includes elements leading to voltage sharpening on the gas discharge gap of a single-barrier discharge. A planar atmospheric-pressure plasma jet with a width of up to 3 cm and length of up to 4 cm has been obtained at the following parameters of the exciting voltage pulse: $\tau = 1\text{--}1.5$ μs , $f = 90$ kHz, and $U_A < 10$ kV. The gas flow rates through the gap were up to 1 L/min.

It has been demonstrated using the *Staphylococcus aureus* culture as an example that the obtained plasma is a source of chemically active particles providing a pronounced inactivation effect.

ACKNOWLEDGMENTS

This study was performed in the framework of the State task for HCEI SB RAS, project no. 13.1.3.

REFERENCES

1. G. Lloyd, G. Friedman, S. Jafri, G. Schultz, A. Fridman, and K. Harding, *Plasma Process. Polym.* **7** (3–4), 194 (2010).
2. A. Schutze, J. Y. Jeong, S. E. Babayan, J. Park, G. S. Selwyn, and R. F. Hicks, *IEEE Trans. Plasma Sci.* **26**, 1685 (1998).
3. M. G. Kong, G. Kroesen, G. Morfill, T. Nosenko, T. Shimizu, J. van Dijk, and J. L. Zimmermann, *New J. Phys.* **11**, 115012 (2009).
4. X. Li, W. Bao, P. Jia, and C. Di, *J. Appl. Phys.* **116**, 023302 (2014).
5. J. Tang, S. Li, W. Zhao, and Y. Duan, *Appl. Phys. Lett.* **100**, 253505 (2012).
6. H. M. Joh, S. J. Kim, T. H. Chung, and S. H. Leem, *Appl. Phys. Lett.* **101**, 053703 (2012).
7. E. A. Sosnin, E. Stoffels, M. V. Erofeev, I. E. Kieft, and S. E. Kunts, *IEEE Trans. Plasma Sci.* **32**, 1544 (2004).
8. M. Laroussi, *Plasma Process. Polym.* **2**, 391 (2005).
9. Y. Daun, C. Hung, and Q. S. Yu, *IEEE Trans. Plasma Sci.* **33**, 328 (2005).
10. T. Shao, C. Zhang, R. Wang, Y. Zhou, Q. Xie, and Z. Fang, *IEEE Trans. Plasma Sci.* **43**, 726 (2015).
11. X. L. Deng, A. Yu. Nikiforov, P. Vanraes, and Ch. Leys, *J. Appl. Phys.* **113**, 023305 (2013).
12. D. A. Lacoste, A. Bourdon, K. Kuribara, K. Urabe, S. Stauss, and K. Terashima, *Plasma Sources Sci. Technol.* **23**, 062006 (2014).
13. E. A. Sosnin, V. A. Panarin, V. S. Skakun, V. F. Tarasenko, D. S. Pechenitsin, and V. S. Kuznetsov, *Tech. Phys.* **61**, 789 (2016).
14. E. A. Sosnin, V. A. Panarin, V. S. Skakun, V. F. Tarasenko, D. S. Pechenitsin, and V. S. Kuznetsov, *Proc. SPIE* **9810**, 98101I (2015).
15. R. F. Mengaliev and M. Yu. Dorogushin, RF Patent No. 2229692 (2002).
16. J. Mahoney, W. Zhu, V. S. Johnson, K. H. Becker, and J. L. Lopez, *Eur. Phys. J. D* **60**, 441 (2010).
17. *Plasma for Bio-Decontamination, Medicine and Food Security (NATO Science for Peace and Security Series A: Chemistry and Biology)*, Ed. by V. Zdenko, K. Hensel, and Yu. Akishev (Springer, Dordrecht, 2012).

Translated by A. Nikol'skii